Chapter 1

Introduction

1.1 Overview

This chapter provides an introductory overview of magnetic phenomena, which are essential for understanding the present work. The competition between various magnetic interactions gives rise to the formation of different ground state spin configurations, such as spin spirals, 120°-spin structures, domain walls, magnetic skyrmions, and multi-q states; the obtained experimental results are presented in chapter 4, 5 & 6. First, the exchange interactions and magnetic anisotropies are introduced, which are responsible for noncollinear magnetism. Thereafter, various magnetic ordering and spin structures are introduced.

1.2 Magnetic interactions of interest

Recently, noncollinear magnets have become a new research interest of investigators; they form a background for various exotic magnetic phases. This section emphasises various magnetic interactions of importance, which are key players in noncollinear magnetism, sometimes competing together. The magnetic nature of any magnetic specimen depends on the mutual strength of the associated interactions between the moments of the magnetic ions present in it. The associated interactions [1] are described below.

1.2.1 Exchange interaction

Exchange interactions are the essence of magnetism, responsible for long-range magnetic order, and depend on the spatial arrangement and interatomic separation of localised magnetic moments in solids. It is purely quantum mechanical entity, because the electrons

are indistinguishable particles. First, in 1928, Heisenberg demonstrated the origin of a substantial molecular field, which is answerable for parallel alignment (↑↑) of spins in the domains of ferromagnetic specimens [2].

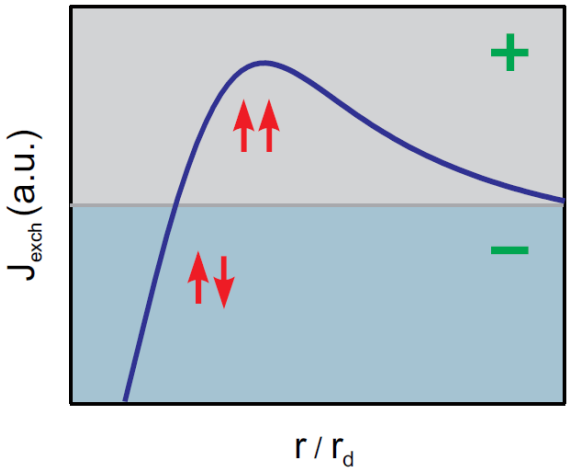

Fig. 1.1 Bethe-Slater representation, showing the dependence of sign of J_{exch} (exchange coefficient) to the ratio of r (interatomic distance) and r_d (radius of the unfilled d shell) in case of direct exchange coupling (adapted from reference [3]. A (- ive) value of the J_{exch} results in an ↑↓ (antiferromagnetic) ground state arrangement of spins, whereas a positive value leads to a ↑↑ (ferromagnetic) ground state coupling, which is indicated by red arrows.

Microscopically, the exchange interaction between two electrons results from the Coulomb interaction associated with the Pauli exclusion principle. Therefore, the overall wave function of a system with two electrons must be antisymmetric considering the exchange of electrons. Therefore, the spatial part of the wave function is symmetric (triplet), the spin part must be anti-symmetric (singlet), and vice versa.

Thus, for a single pair of magnetic moments, the spin-dependent term in the effective Hamiltonian ($\mathscr{H}^s$) [1] can be written as:

$$\mathscr{H}^s = -J_e \overrightarrow{S_1}.\overrightarrow{S_2} \tag{1.1}$$

where J_e is the exchange parameter (also called an exchange coupling constant) that describes the strength of the coupling of the pair of interacting spins ($\overrightarrow{S_1}$ & $\overrightarrow{S_2}$). This model can be extended to a crystal lattice structure with multiple - electrons, and the exchange

energy is given by the Heisenberg Hamiltonian, which involves the sum over all pairs of spin:

$$\mathscr{E}_{exch} = -\sum_{ij} J_{ij}\overrightarrow{S_i}\cdot\overrightarrow{S_j}\;; \quad whereas \quad J_{ij} = \begin{cases} J & for\ nearest\ neighbor\ spins \\ 0 & otherwise \end{cases} \tag{1.2}$$

where J_{ij} is the exchange integral, and the strength of J_{ij} degrades rapidly with the separation between the atoms [3]. Based on inter-atomic distances, *i.e.*, orbital overlap, the values of J_{ij} might have a positive or negative sign, resulting in the parallel or antiparallel ground state configuration of spins, respectively, as shown in Fig. 1.1. Often, a good approximation of J_{ij} is given by Eq. 1.2, which holds for the next neighbour exchange interaction, *i.e.*, short-range direct exchange interaction. If the interatomic separation is too large, *i.e.*, the overlapping of the wave-function is too small, and the direct exchange coupling is not strong enough to overcome thermal excitations, which gives rise to paramagnetic behaviour. In the case of metals, above a certain distance, the exchange interaction no longer results from the direct overlap of the electron wave-function. However, it interacts with conduction electrons (Ruderman-Kittel-Kasuya-Yoshida (RKKY) interaction [4–6].

The evaluation of magnetic theory has led to the prediction of various types of exchange coupling between neighbouring spins, namely direct and indirect exchange coupling. Direct exchange coupling occurs between neighbouring magnetic moments that have overlapping wave functions [3]. The indirect exchange reveals the coupling of magnetic moments over relatively large distances, and there is no direct overlap between neighbouring electrons, which might be mediated through different mechanisms depending on the material systems under consideration. This section is basically focuses on the Heisenberg model, an example of an interaction known as direct exchange coupling.

1.2.2 Dzyaloshinskii-Moriya interaction

Dzyaloshinskii-Moriya interaction (DMI) is an anisotropic antisymmetric exchange interaction between two neighbouring magnetic moments, resulting from the complex interplay between lack of inversion symmetry and spin orbit coupling (SOC). The theory was first proposed by Dzyaloshinskii [7], and later the role of SOC through nonmagnetic ligand, called anisotropic superexchange interaction, was described by Moriya [8] to study the weak ferromagnetic (canted antiferromagnetic) nature of α-Fe_2O_3. The energy corresponding to the two neighbouring magnetic moments $\overrightarrow{S_p}$ and $\overrightarrow{S_q}$ can be expressed as

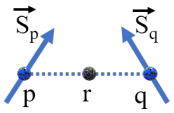

Fig. 1.2 Schematic representation of a system with two spins are used to discuss the DMI.

$$\mathscr{E}_{DM} = \vec{D} \cdot (\vec{S_p} \times \vec{S_q}) \tag{1.3}$$

where $\vec{S_p}$ and $\vec{S_q}$ are the spins of two interacting magnetic ions, and $\vec{D}$ is a constant known as the DM vector. In contrast to the aforementioned exchange interaction, this favours non-collinear spin ordering. Because the interaction is antisymmetric, it vanishes if it possesses inversion symmetry in the system.

The direction of the $\vec{D}$ vector can be determined from the symmetry rule summarised by Moriya [8] with a similar sketch, as shown in Fig. 1.2. He considered two magnetic moments, $\vec{S_p}$ and $\vec{S_q}$, which are located at positions p and q, respectively, and the point bisecting the straight line pq is denoted by r. He proposed the following symmetry rules:
• When the centre of the inversion is positioned at r, $\vec{D} = 0$.
• If the mirror plane $\perp$ (pq) passes through r, then $\vec{D}$ is $\perp$ (pq).
• When there is a mirror plane including p and q, then $\vec{D}$ is $\perp$ this mirror plane.
• If there is a two-fold rotation axis $\perp$ (pq) passes through r, then $\vec{D}$ is $\perp$ the two-fold axis.
• When there is an n-fold rotation axis $\parallel$ (pq), $\vec{D}$ is parallel to (pq).

In bulk systems, this broken inversion symmetry can be considered as an intrinsic property of the crystal structure, for example, in B20 compounds such as MnSi [9] or can be induced by distortion of the lattice, such as in some multiferroic orthoferrites and orthochromites [10, 11]. For the particular B20 compounds, the D vector is oriented parallel to the direction of joining the sites, where the two spin moments are positioned, and the configuration is often called bulk DMI.

In the case of ultrathin films, the symmetry is broken at the interfaces and the direction of the $\vec{D}$ vector changes depending on the symmetry of the surface. The strength of the DMI was directly proportional to the intensity of the SOC in the system. Consequently, systems with larger DMI are often arranged such that an interface is in between the nonmagnetic heavy metal layer and magnetic thin film. The DMI is associated with a heavy metal atom having a large SOC for each pair of moments in the magnetic layer, which is positioned opposite to the interface. All these effective contributions determine the value of the $\vec{D}$ vector and its orientation.

1.2.3 Magnetic anisotropy

Most of the existing natural or artificial magnetic materials exhibit inherent magnetic anisotropy, *i.e.*, the free energy linked with the magnetisation depends on the direction in which the field is applied, and in the absence of a field, the magnetisation will align along the preferred crystallographic direction. The energy is minimum along an easy axis, and a large value of the applied field is required to orient the magnetisation in order to reorient in another direction, the so-called hard axis. For the magnetic anisotropy, the structural symmetry results in magneto-crystalline anisotropy, and the surface morphology, grains, and stresses within the crystals are supposed to be a source of anisotropy, as studied by Sander *et al.* [12]. The preferred orientation of the magnetisation vector of a ferro/ferri/antiferromagnet material, therefore, results from the competition among various energies, which is expressed as follows:

• **Exchange energy:** minimized if classically spins are aligned $\parallel$ to each other.

• **Zeeman energy:** minimises if spins are aligned $\parallel$ to the applied external field;

• **Uniaxial anisotropy energy:** minimised if the magnetic moments are aligned along the easy axis.

• **Thermal energy:** attempts to randomise the spin magnetic moments;

• **Magnetostatic energy:** is minimised if the magnetisation pointed in the direction of the magnetic dipole moment fields created at the interfaces of the specimen, such as the domain wall formation.

Microscopically, the spins are coupled with the electric field that arises due to the charge density of the surrounding electron, *i.e.*, the so-called crystal field through the SOC, and their energy. Therefore, depends on their absolute orientation concerning the crystallographic axis, as well as their relative orientation with respect to one another. Such a local dependency, so-called single-ion anisotropy (SIA), or simply magneto-crystalline anisotropy [13]. To minimise the magneto-crystalline energy, a crystal may undergo a small deformation when magnetised, and if not allowed to expand freely, may be a source of internal stress in the crystal system. In contrast, the application of stress to a crystal system will affect the lattice and hence the magnetocrystalline energy.

1.2.4 Competing exchange interaction in 1D-chain

Above large atomic distances, the exchange interaction becomes very small, and in many systems, it is worth considering the nearest-neighbor interactions described by the coupling constants. Here, one-dimensional spin chain considered with coupling between the nearest neighbour (NN) interaction J_1 is FM, and the next-nearest neighbour (NNN) interaction

J_2 is AFM (see Fig. 1.3 (a)), the exchange coupling can be frustrated and allows to stabilize non-collinear spin structures (described in next sections). Apart from competing interactions, such frustration of the exchange coupling can also occur in a geometrical sense, for example, in the case of AFM coupling on a triangular spin-lattice (see Fig. 1.3 (b)). In this case, the ground state is achieved by a forming Néel state in which the angle between adjacent moments is 120°, the so-called 120° spin structure (shown in the next section) [14–16].

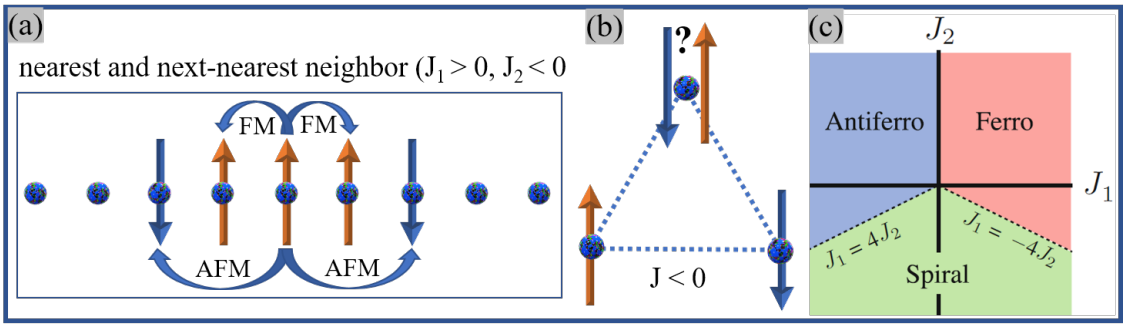

Fig. 1.3 Typical sketches of (a) 1-D chain of spins with competing J_1 and J_2 interactions in the centrosymmetric system, (b) Geometrical frustration of the triangular spin-lattice (odd loop of AFM coupling), and (c) Phase diagram showing magnetic ground state for J_1-J_2 model, and Fig. (c) was adopted from [17].

The corresponding microscopic spin Hamiltonians $\mathscr{H}_c$ for a centrosymmetric system in a 1D-chain model can be described as follows:

$$\mathscr{H}_c = -J_1 \sum_{NN} \overrightarrow{S_i} \cdot \overrightarrow{S_j} - J_2 \sum_{NNN} \overrightarrow{S_i} \cdot \overrightarrow{S_k} \tag{1.4}$$

where $\sum_{NN}$ and $\sum_{NNN}$ exhibit the sum over the NN and NNN, respectively, [17]. With only NN interaction, which is FM in nature, the ground state of such a system is collinear with the adjacent lattice. On the other hand, competing interactions such as J_2 are negative, *i.e.*, AFM, neither FM nor simple AFM spin arrangement can satisfy the second term, and thus magnetic frustration arises [17, 18].

By introducing a generalised spin order and analyse the condition to satisfy $d\mathscr{H}_c/d\theta = 0$, one can find the length scale of the spin modulation of the magnetic ground state (q).

$$q = [\{\cos^{-1}(-J_1/4J_2)\}/a] \tag{1.5}$$

where a is the lattice parameter of the crystal lattice. Provided the conditions $J_2 < 0$ and $(-1 \leq \cos(q) \leq 1)$ is satisfied, the spiral magnetic order is more stable than the FM

or simple AFM order. The spin spiral period depends on a delicate balance of the ratio (J_1/J_2)[19]. The order of magnitude of J_1 and J_2 can be the same, which may result in a spin modulation wavelength on the order of less than $\sim$ 10 nm[18]. The corresponding phase diagram of the J_1-J_2 model is shown in Fig. 1.3 (c) [17, 19].

1.3 Magnetic order and spin structures

In this section, a brief discussion of the various magnetic structures as a function of atomic structure and exchange interactions is presented. The lack of atomic ordering and the multi-sublattices characteristic of disordered and amorphous materials make them have complex magnetic structures [20], which is given below:

1.3.1 Spin structures in pure crystals

Investigations on crystalline materials have played an excellent role in conventional solid-state material science. The magnetic ordering in pure crystals without any site disordering is not always consistent [21]. For instance, Fig. 1.4 shows the complex spin structures in pure crystals that have been worthily evaluated by Keffer [21, 22]. These coherent noncollinear spin structures generally arise because of competing interactions, regardless of whether these can be exchange interactions (symmetric and antisymmetric) having one or more shells of nearest neighbours or exchange and magneto-crystalline anisotropy.

Commensurate spin structures

Materials in nature, microscopic or macroscopic, have their own physio-chemical properties, which strongly depend on their atomic structures. Therefore, structure determination is extremely important in condensed matter physics, chemistry, and materials science. In condensed matter physics, there are many models of phase transitions successfully demonstrated for a more ordered and less ordered state [66, 133, 142]. If the dimension of the magnetic unit cell is equal to the integer multiple of the nuclear unit cell, the magnetic structure is commensurate. The magnetic structure is incommensurate when the magnetic unit is an irrational multiple of the nuclear unit cell. Incommensurate spin structures may be linear but quite complicated, like a spiral, cycloidal, conical, umbrella, etc. Especially in rare-earth compounds, very complex magnetic structures have been found, which are demonstrated in the next section [21, 38, 48, 62].

Incommensurate helical spin structures

Magnetism due to helical spin structure, called helimagnetism, was first proposed in 1959 in MnO_2 [23] by means of neutron diffraction, and real space visualisations of helical spin order were first achieved in metal silicide by Lorentz electron microscopy. Most of the materials exhibit helical ordering at a range of low temperatures, whereas in 2017, Lancaster *et al.* reported some helimagnetic structures, which are stable at room temperature [24].

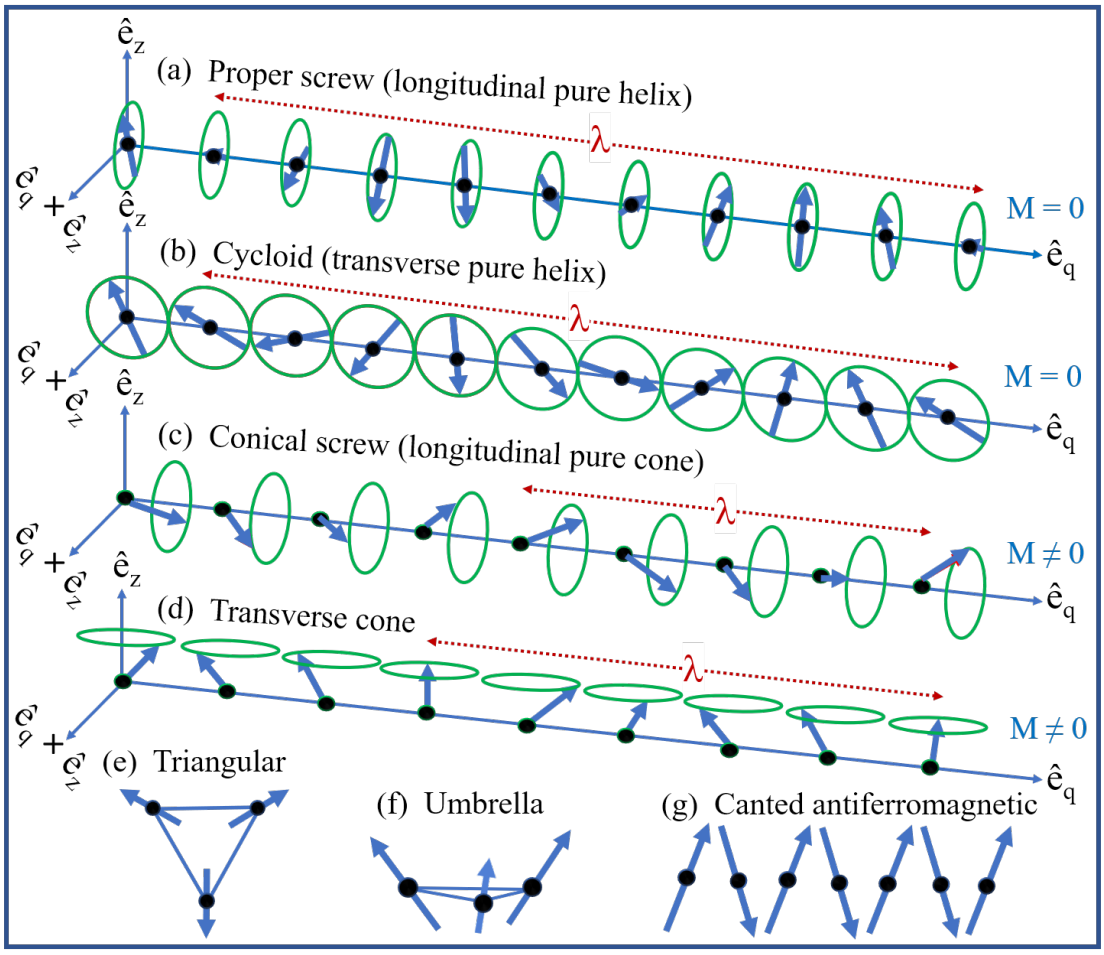

Fig. 1.4 Sketches of some noncollinear spin structures found in pure crystals: (a-d) coherent helical magnetic structures with period of spin spiral (λ); (a) proper screw (longitudinal pure helix), (b) cycloidal (transverse pure helix), (c) conical screw (longitudinal pure cone) (d) transverse conical (e) three-sublattice classical 120° spin structure, (f) umbrella kind of spin structure, and (g) canted antiferromagnet (weak ferromagnet).

Incommensurate helical spin structures often arise from a delicate balance between the competing exchange interactions (see section 1.2.4) in binary transition metals or rare-earth metals with hcp structures that exhibit a layered crystalline structure with a stacking sequence of AB or ABC, which is characterised by parallel alignment of the moments within each layer, *i.e.*, each plane shows ferromagnetic ordering [15, 25, 26]. However, the rotation of the magnetisation differs by the angle α from layer to layer. To describe various types [27–29] of the two essential features of the helical spin order, one of them is the unit vector ($\hat{e}_q$) along the direction of the modulation vector (q), and the second is the orientation of the spin spiral plane, in which rotation of spins takes place. Fig. 1.4 (a-d) illustrates the typical helical spin structures along with an array of magnetic ions [17]. The spin spiral plane $\perp$ (Fig. 1.4 (a)) and $\parallel$ (Fig. 1.4 (b)) to the ($\hat{e}_q$) vector, characterize the proper-screw (longitudinal pure helix) and cycloidal (transverse pure helix) or spiral structure, respectively. Both the helical and spiral spin orders correspond to zero net magnetic moments. In addition to their antiferromagnetic nature, a conical screw (longitudinal pure cone) (Fig. 1.4 (c)) and transverse conical spin structure (Fig. 1.4 (d)) exhibit a net magnetization in the direction $\parallel$ q vector and $\perp$ to q, respectively [17, 18]. These spin helices generally evolve by applying weak magnetic fields to helical or cycloidal spiral structures.

Another underlying but interesting class is the triangular spin-lattice (see Fig. 1.3 (b), the frustration in these systems often gives rise to the noncollinear (or noncoplanar) spin structures due to competing interactions. The resulting ground-state spin configurations are presented in Fig. 1.4 (e & f), corresponding to well-known co-planer 120° spin structure and noncoplanar umbrella-like spin structure, respectively. In the case of the 120° spin structure, three antiferromagnetically coupled spins are located at each corner of a triangle and make an angle equal to $\pm$120° with the neighbourhood spins, whereas the top view of the umbrella structure is also a 120° spin structure. Both the structures in the triangular spin-lattice occur owing to the delicate balance of exchange anisotropy (J/Jz) and field strength (H) [30]. For a more detailed description, refer to [26, 30]. In the case of complete AFM ordering, all the moments are identical, and the cancellation of moments leads to a zero net magnetic moment. A special type of AFM ordering leads to a non-zero net magnetic moment, so-called canted antiferromagnetic ordering, in which neighbouring moments are misaligned by some angle (see Fig. 1.4 (g)) [31]. Owing to the slightly canted nature of moments, a complete cancellation cannot be achieved; although the spin structure is antiferromagnetically ordered, it will exhibit a net residual moment by means of weak DM interaction represented by Eq. 1.3 [32]. Such a material is called a canted antiferromagnet (or equivalently, a weak ferromagnet) [33, 34].

1.3.2 Spin structures in disordered and amorphous materials

Apart from the above overview of coherent noncollinear spin structures found in pure crystals, one does not think it is hard to visualise the partially random or incoherent spin structures found in disordered crystals. The possibility of randomly canted spin structures was ingrained in the mid-1960s to be deeply alluded by Morrish [21]. This section discusses the incoherent spin structures in partially disordered and fully disordered (amorphous) systems are investigated. Modifications of collinear spin structures in partially and fully disordered systems that can be introduced by crystal surfaces and solid solutions, mainly focusing on systems with frustrated antiferromagnetic interactions.

Crystal surfaces

Crystal surfaces are a truncation of the bulk crystalline lattice at the nanoscale; the various properties of the crystal surfaces are strongly dependent on the arrangement of atoms on the surface. Surfaces act as imperfections in pure crystals [21]. In the field of nanomagnetism, most phenomena occur either at or near surfaces owing to the finite size effect and surface effects, which result from the high surface-to-volume ratio and the symmetry breaking of the crystal structure at the surface and/or interface, respectively, [35, 36]. A nexus between finite-size and surface effects governs the magnetic properties of ultra-fine layered magnetic systems, whose importance is inversely proportional to the thickness [36]. Various types of surface defects exist, such as lowering the atomic coordination, atomic vacancies, and lattice disorder that lead to surface spin disorder and frustration. Subsequently, the magnetic structure at the surface layer is usually significantly different from that in the body of nanoparticles, and the magnetic interactions in the surface layer have a noticeable effect on the magnetic properties of the nanoparticles [37]. Surface effects dominate the magnetic properties of the smallest particles because decreasing the particle size increases the ratio of surface spins to the total number of spins [36]. Indeed, surface effects can lead to a decrease in the magnetisation of small particles (< 100 nm) of γFe_2O_3, with respect to the bulk value [35, 38]. This reduction has been associated with distinct mechanisms, such as the existence of canted spins, a magnetically dead layer on the surface, randomly oriented noncollinear surface spins, and spin-glass-like behaviour [39, 40]. The disordered crystal structure results from the high surface curvature [41], which increases as the particle size decreases, modifying the magnetic moment of surface atoms and anisotropy, which results from surface anisotropy [42].

Solid solutions (mixed crystals)

Some materials are used to form crystals, comprising atoms of two or more different substances, which are called solid solutions (or referred to as mixed crystals). In the case of solid solutions, not only the molecular structure should be of the same type, but also essentially, the crystal lattices must be of the same type and have similar dimensions [43]. There are no possible solid solutions (mixed crystals) that are of great significance compared to pure end-members, and there is a huge amount of literature available on their magnetic properties. The scheme for the generation of random magnetic structures, all of which involve random stacking of the deck with a delicate balance of competing interactions [21], which includes the following:
(1) Diluting ordinary magnets with nonmagnetic impurities to alter the balance of competing exchange interactions in a random way.
(2) Preparation of solutions of two different magnets like FM and AFM.
(3) Introducing impurities into noncollinear magnets.
(4) Preparation of solid solutions between final products with incompatible spin structures.

The majority of solid solutions presents are of what is called the substitution type. These solutions are obtained by replacing some of the atoms in the crystal lattice of the primary substance with the atoms of the other substance. The obtained magnetic structures are characterised by their range of spin correlations [21, 44].

Collinear spin structures in disordered and amorphous materials

Now, begin with considering the scheme (1) to the collinear magnets in disordered systems, and so-called as dilute magnets are characterized by random exchange interactions without frustration [45]. Diluting a compound with complete ferromagnetic or antiferromagnetic exchange interactions by substitution of nonmagnetic ions does not destroy ferro/ferri/antiferro-ordering in the bulk cluster, as long as the concentration of magnetic ions exceeds the substituted one (see Fig. 1.5 (a)) [46, 47]. From a theoretical approach, the dilute ferro/ferri/antiferro can be described by random exchange interactions, *i.e.*, interaction varies only in strength and not in sign. The ground state of dilute ferro/ferri/antiferroo is qualitatively the same as that of pure systems [45].

As a guide to discussing magnetism in non-crystalline solids, it is crucial to address the broad categories of spin ordering in amorphous solids. In contrast to collinear spin ordering in disordered systems, it is important to discuss the collinear spin ordering encountered in amorphous materials. A crucial feature of the magnetic order for each case is comprehended as a component of the magnetic moment of each atom as constant with

respect to time, *i.e.*, $\overrightarrow{S_i} \neq 0$, where $\overrightarrow{S_i}$ and is the time average of the spin moment, with similar magnetic interactions [48].

Fig. 1.5 (a) collectively represent the collinear spin ordering in disordered and amorphous solids (in brackets) having non zero net magnetic moment, corresponding to ferromagnetic, ferrimagnetic and zero magnetic moments corresponds to antiferromagnetic spin order, respectively [21, 46, 48].

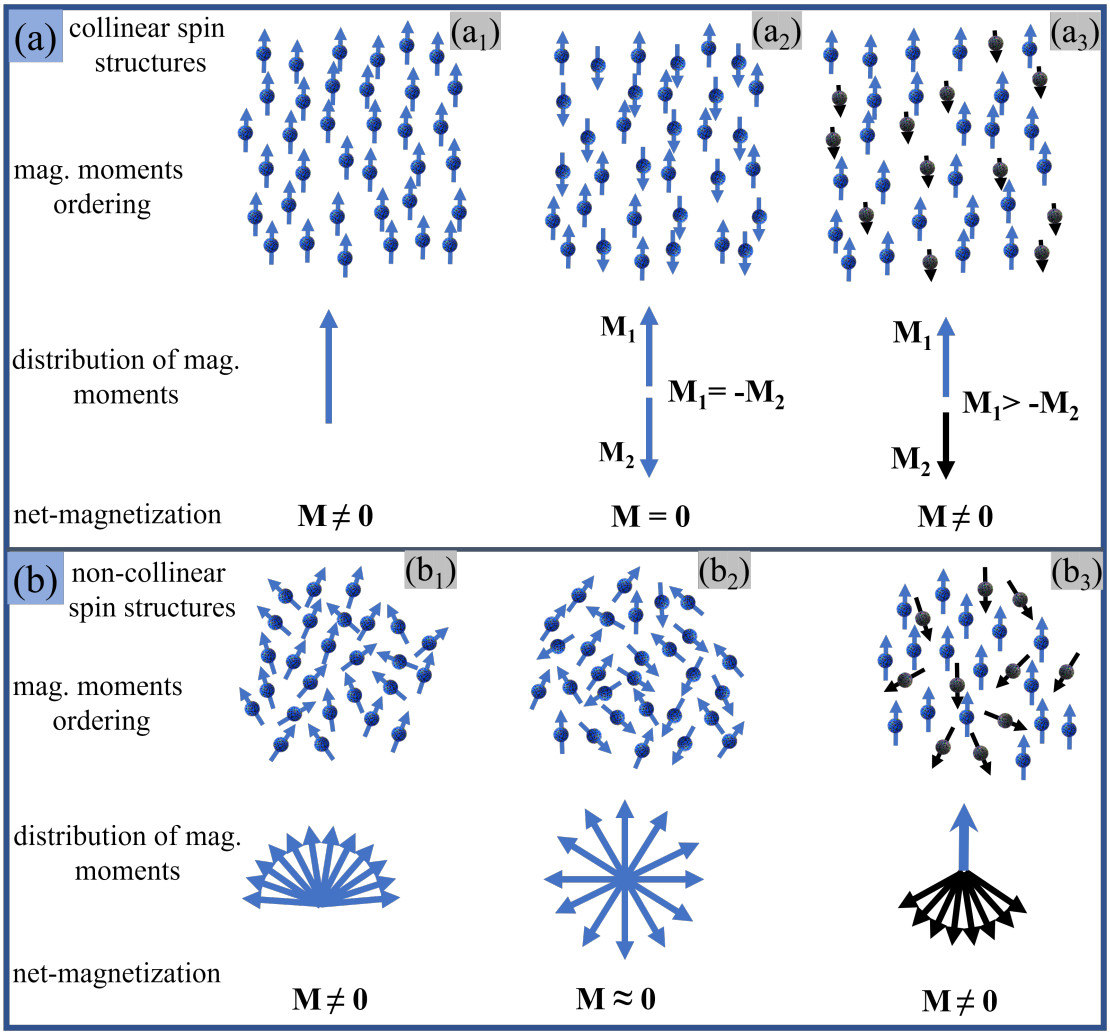

Fig. 1.5 Sketches of some random collinear and noncollinear spin structures (a & b) found in disordered and amorphous materials (in brackets): (a_1) dilute FM (random collinear FM), (a_2) dilute AFM (random collinear AFM), (a_3) dilute FI (random collinear FI), and (b_1) randomly canted FM (asperornagnet), (b_2) spin glass (speromagnet), (b_3) randomly canted FI (sperimagnet). The bottom part of each Fig. represents the angular distribution of the spin moment orientations.

Noncollinear spin structures in disordered and amorphous materials

In addition to the familiar collinear magnetic structures briefly introduced in the preceding paragraph, the classification of random noncollinear spin structures in disordered solid is demonstrated below [21, 48]. Fig. 1.5 (b) illustrates the variety of noncollinear spin ordering phenomena in materials in disordered and amorphous materials. Depending on the values for the exchange and the local anisotropy randomly canted AFM (asperomagnet), spin glass (speromagnet) and randomly canted FI (sperimagnet) configurations are possible as outlined in Fig. 1.5 (b), respectively [20, 21, 48].

There are various classes of two-sublattice structures that can be distinguished. In the case of collinear spin, structures are FM/FI or AFM, depending on whether the sublattices are coupled parallel or antiparallel. If one or both sublattices possess a random, noncollinear structure but have a net magnetisation, the structure will be termed sperimagnetic in amorphous and randomly canted FI in disordered systems [49]. If both sublattices exhibit random noncollinear structures with a vanishing net moment, the structure is once again speromagnetic.

1.3.3 Spin orderings in perovskites

Apart from the aforementioned magnetic structures, rare-earth orthoferrite ($RFeO_3$) perovskites are a family of canted antiferromagnets [50]. The main leading interactions are isotropic exchange interactions among the nearest neighbour (NN) moments [11]. Depending on the relative sign of NN interactions, five types of collinear ordering emerge, which are discussed below and shown in Fig. 1.6 (i-m).

• **F-type**: all magnetic moments are pointed in the same direction, that is, complete FM ordering.

• **A-type**: the intra-plane coupling of moments is FM, whereas inter-plane coupling is AFM, *i.e.*, the moments are directed in opposite directions in successive planes.

• **C-type**: the moments are aligned in opposite directions in consecutive lines, *i.e.*, AFM ordering of the FM chains.

• **G-type**: the NN moments are pointed in opposite directions, *i.e.*, complete AFM ordering.

• **E-type**: This is a specific type of collinear magnetic order with intra-plane spin up-up down-down (uudd) AFM order and inter-plane spins aligned antiparallel, *i.e.*, within plane moments form "zig-zag" lines of parallel moments and stacked antiferromagnetically next to each other. This type of magnetic order is realised in rare-earth manganites ($RMnO_3$) as a result of spin-phonon coupling beyond the nearest-neighbor coupling [51–

53]. Interestingly, such collinear ordering already breaks the inversion symmetry and has been predicted theoretically and experimentally to induce an electric polarisation [10, 54].

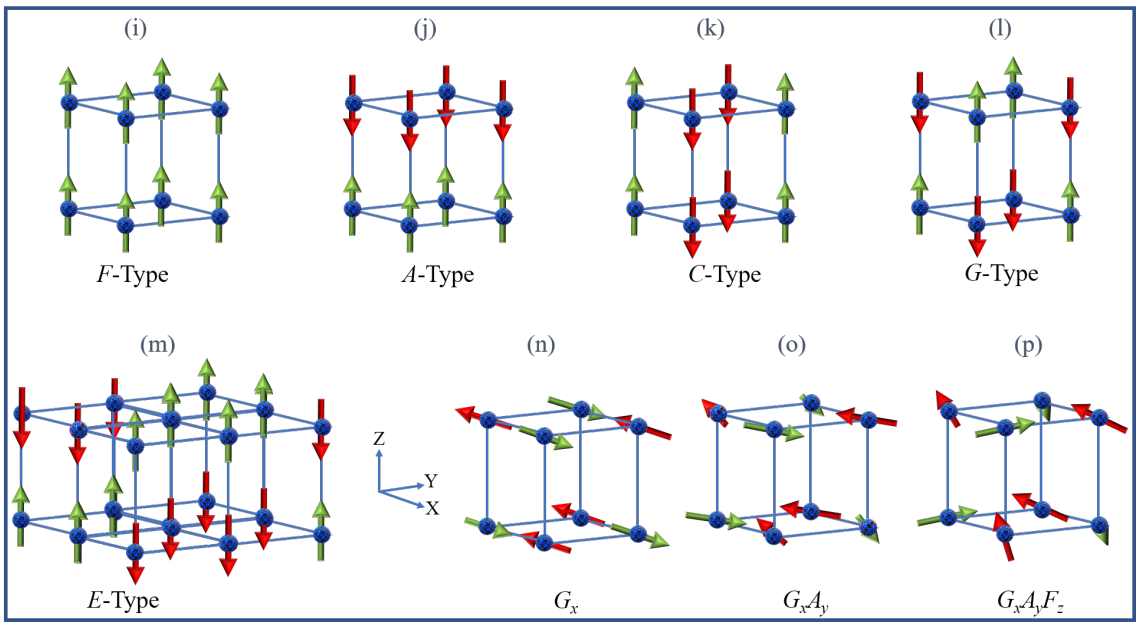

Fig. 1.6 Schematic drawing of collinear spin order of (i) *F*-type, (j) *A*-type, (k) *C*-type, (l) *G*-type and (m) *E*-type (for the sake of simplicity, the spins are directed along the z-axis) and (n) G_x, (o) p_xA_y and (h) $G_xA_yF_z$ represent non-collinear spin orders in cubic perovskites.

Bertaut [55] describes a very common notation to describe the noncollinear nature of spins in perovskite. In this notation, the spin structure is denoted by specifying the type of magnetic order (such as A, F, C, and G) displayed along each of the principal crystallographic directions as $M_x^{'}M_y^{''}M_z^{'''}$, where $M^{'}$s represent different magnetic order [56]. For instance, simply assume a G-type structure in which the spins are aligned parallel to the x-axis. In Bertaut's notation, this is represented as G_x (as shown in Fig. 1.6 (n)). If this order represents an additional A-type spin component parallel to the y-axis, then it is represented as G_xA_y (as shown in Fig. 1.6 (o)). If there is one more F-type spin component parallel to the z-axis, then the overall structure is represented as $G_xA_yF_z$ (as shown in Fig. 1.6 (p)) and called as Γ_4 spin structure. Most perovskites with the Pbnm structure possess such spin structures. This is a convenient notation for the description of spin orders in perovskites.

1.4 Phase diagram for competing interaction in triangular lattice

Apart from the geometrical magnetic frustration illustrated above, the noncollinear spin structure in layered triangular systems often results from the presence of competing ferromagnetic (FM) and antiferromagnetic (AFM) Heisenberg exchange interactions between spins [25, 57–59]. Considering $J_1 - J_3$ & $(J_1 - J_2)$ model in a magnetic field of strength (H) for a triangular spin-lattice, the Hamiltonian (H) can be expressed as

$$\mathscr{H} = -J_1 \sum_{<i,j>} S_i.S_j - J_{2,3} \sum_{<<i,j>>} S_i.S_j - H \sum_i S_i \tag{1.6}$$

where $\sum_{<i,j>}$ and $\sum_{<<i,j>>}$ exhibit the sum over the nearest neighbours (*nn*) and next-nearest neighbours (*nnn*), respectively, which are shown in Fig. 1.7 (a). The third is the Zeeman energy, which was discussed in the previous section [25]. With only nn interactions, which are antiferromagnetic in nature, the ground state of such a system is commensurate to the adjacent lattice. On the other hand, competing interactions such as $J_1 > 0$ and the AF third-neighbor interaction $J_3 < 0$ with $J_1|J_3| < 4$, an incommensurate ground state appears [25, 26].

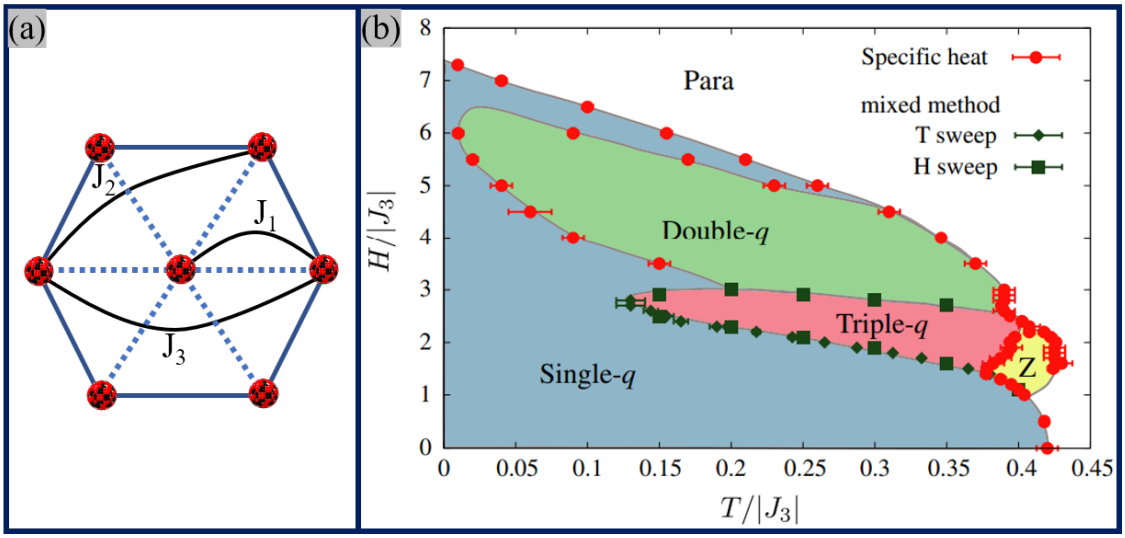

Fig. 1.7 (a) Competing nearest neighbor exchange interactions, J_1 (first), J2 (second), and J3 (third), in a triangular lattice, and (b) Magnetic phase diagram of competing interaction (Eq. (1.6)) with J_1/J_3 = -1/3 in the $H - T$ plane, obtained from the simulations. Fig. (b) was adopted from Okubo *et al.*[60].

In other words, when nnn interaction becomes dominant, the ground state often results in an incommensurate spiral structure. In such a compound, the magnitude of the antiferromagnetic nnn interaction is larger than that of the ferromagnetic nn interaction. In the presence of an externally applied magnetic field, the ordered state of the sublattice structure is robust and leads to an exciting phase diagram as a function of temperature [25, 26, 61–63], which is shown in Fig. 1.7 (b) represent the normalized $H-T$ phase diagram obtained from Monte Carlo simulation method. Apart from the single-q spiral ground state, the triple-q skyrmion-lattice (SkL) phase appears at a definite temperature range under a magnetic field. Owing to the presence of space-reflection symmetry on the xy spin components, the SkL and antivortex-type SkL states are degenerate [18, 60].

1.5 Materials under study

The investigated materials are $NiBr_2$, Cd-doped Cu_2OSeO_3, and $SmFe_{3/4}Mn_{1/4}O_3$ single crystals from different families of the crystal system, one of them is transition metal dihalides (MX_2, where M (metal cation), X (halogen anion)), Cd-Cu_2OSeO_3 is the Skyrmion host material, and the other is a rare earth orthoferrite ($ReFeO_3$, where Re is a rare-earth element). Both MX_2 [18, 64] and $ReFeO_3$ [11, 65] have long been studied as prototypes of itinerant antiferromagnets with collinear and noncollinear magnetic ground states, with triangular lattice and perovskite lattice structures, respectively. Apart from collinear antiferromagnetically coupled materials, both lattice structures are particularly interesting in terms of noncollinear spintronic materials, which have attracted considerable research attention owing to exotic physical phenomena [66]. In the following subsection, briefly introduction of investigated materials is demonstrated.

1.6 Transition metal dihalides: $NiBr_2$

In transition metal dihalides, $NiBr_2$ is a typical example of a triangular spin-lattice of a chiral magnet that exhibits a temperature-driven phase transition from a commensurate antiferromagnetic to an incommensurate spin helix phase. This has attracted significant attention owing to the discovery of exotic magnetic states, such as the formation of multiple-q states, as theoretically predicted by Okubo *et al.* [60] because of the presence of incommensurate spin structures and multiferroicity [17, 67–69]. In the triangular spin-lattice of $NiBr_2$, a modulated spin structure arises owing to the presence of competing exchange interactions along with magnetic anisotropy [17, 67]. Few investigations have been carried out to understand the microscopic source of incommensurate ordering that is

responsible for helimagnetism in the spin triangular lattices of $NiBr_2$ [59, 68]. However, in multiferroic helimagnets, enhanced understanding to control and modify spin helices in incommensurate phases at the nanoscale further needs to be established that have high technical implications for realising next-generation energy-efficient data storage devices [66, 69]. Detailed magnetic and crystallographic information is provided in the introduction of chapter 4.

Our work demonstrates that by combining state-of-the-art neutron scattering experiments with magnetisation measurements, microscopic information in a triangular spin system can be assessed. These experimental observations (given in chapter 4 & 5) will further accelerate the search for exotic quantum states in helimagnetic systems. Our work could be foreseen as a novel approach for an accurate understanding of the role of neighbouring interactions in triangular spin systems, which paves the way for exploratory research on field-induced phase transitions, where the choice of spin helices and topological magnetic texture will be a tool to improve the performance.

1.7 Magnetic skyrmions: Cd-Cu_2OSeO_3

Magnetic skyrmions are small swirling topological objects in the magnetisation texture, having a helical spin structure with propagation (q)- vectors on the nanometre length scale [70]. Magnetic skyrmions came into existence theoretically over 50 years ago by the British physicist T. H. R. Skyrme [71], but the first experimental realisation was achieved in 2009 on MnSi single crystals [9]. Subsequently, various non-centrosymmetric magnetic materials such as FeGe [72], $Fe_{1-x}Co_xSi$ [73], $Mn_{1-x}Fe_xGe$ [74], and $Co_xMn_{1-x}Si$ [75], have been proposed as skyrmionic host materials. Among the skyrmionic host non-centrosymmetric crystal systems, Cu_2OSeO_3 is a multiferroic and Mott insulator material, which hosts a skyrmionic phase in bulk and thin films [17, 76–79]. Because of these intriguing features among the skyrmionic host materials, Cu_2OSeO_3 is a potential candidate for next-generation energy-efficient magnetic data storage devices. The important criteria of any skyrmion-hosting magnetic materials are the temperature and field range in which the SkL can be alive. This is the first system in which the skyrmionic phase has been experimentally realised in the Mott insulator [17], and shows the room-temperature skyrmionic phase under high pressures, which was recently reported by Deng *et al.* [80]. It has been established that: skyrmion lattice can be tuned using external stimuli such as chemical substitution, pressure, and electric and magnetic fields instead of direct currents in Cu_2OSeO_3, which opens the door to explore ultra-low-power-consuming spintronic devices [71, 81]

This work has demonstrated a systematic strategy for the direct and ultra-fast synthesis of Cd-Cu_2OSeO_3 single-crystalline with nominal doping of Cd along with precursors followed by a one-step quenching process at 600°C with a very slow heating rate. In the case of a conventional solid-state reaction, 600°C for 10 days with intermediate grinding followed by various processes (vacuum-sealing, palletization, etc.) [82], in the case of CVD, 500°C for 6 weeks [17, 71, 79]. Therefore, the present study allows us to develop a time-and cost-efficient strategy to synthesise this kind of complex material. In addition, enhanced optical and magnetic properties of Cd-doped Cu_2OSeO_3 nanocrystalline are reported.

1.8 Rare-earth orthoferrite: $SmFe_{3/4}Mn_{1/4}O_3$

Rare earth orthoferrite ($RFeO_3$) compounds have complex magnetic interactions between the rare-earth (R) and transition metal (Fe) ions, which makes them of immense scientific interest in studying their exotic magnetic properties [65]. Modifying and controlling the phase transition temperatures to enhance the magnetic properties of such compounds would play a significant role in energy-efficient magnetic storage data technology in future spintronics devices [83]. One of the fundamental magnetic properties of most of the $RFeO_3$ compounds is their spin reorientation transition (SR), during which the magnetisation reversal of the Fe^{3+} sublattice takes place from one crystallographic axis to another upon varying the field and temperature [84–86]. Among the family of $RFeO_3$, $SmFeO_3$ shoes multiple transitions, such as SRT in the narrow range of 450 K to 480 K, which is the highest in the $RFeO_3$ family, spin switching at nearly 278 K, H, 300 Oe and compensation temperature nearly at 4 K, H, 300 Oe are observed in $SmFeO_3$ crystals and can be manipulated by the field at room temperature, which makes $SmFeO_3$ a potential candidate for excellent device characteristics [83].

Recently, numerous studies have been performed on doped rare-earth orthoferrite [87], including R-sites and Fe-sites to improve the physical properties of the host compound, such as crystal structure [88], magnetic structure [89, 90], electronic structure [91], photo-luminescence [92, 93]. Therefore, due to the alteration of physical and structural properties, here, Mn^{3+} substituted at Fe^{3+} site, which is best suited on the basis of the Goodenough-Kanamori [94, 95] theory to show superior magnetic properties due to superexchange interactions, which may reveal fascinating magnetic properties and lattice dynamics. Hence, in this thesis, the structural, electric and magnetic properties along with local interactions in the SFMO single crystal are explored through various measurements.

1.9 Motivation

The interplay among the various competing interactions with different hierarchical energy levels makes centrosymmetric noncollinear magnets an interesting class of materials. The experimental and theoretical indication of the possibility of manipulating spin-modulated states and the stabilisation of multiple-q states (not skyrmion state) have pointed out that these systems have the potential for energy-efficient magnetic data storage applications, especially in the field of spintronics. The motivation behind this investigation was to find and study these nanometric length scale exotic states in centrosymmetric crystal systems, which is only theoretically predicted. Prototype chiral multiferroic Mott insulator Cu_2OSeO_3 nanocrystallites.

1.10 Outline of thesis

This thesis presents experimental investigations on $NiBr_2$, Cd-Cu_2OSeO_3, and Mn-doped $SmFeO_3$ single crystals by dc magnetisation, ac susceptibility, small-angle neutron scattering (SANS) measurements along with X-ray absorption spectroscopy (XAS). The main focus is on $NiBr_2$; CSO and SFMO are toward spin reorientation from commensurate to incommensurate magnetic structure and weak ferromagnetic to compensated antiferromagnetic, respectively, at low temperatures, which have immense scientific and technological implications for next-generation energy-efficient magnetic data storage devices.

The thesis consists of the following chapters:

• **Chapter 1:** presents a literature survey of the existing work related to the formation of a helical ground state, formation of complex magnetic structures: multi-q states and magnetic skyrmions and their experimental and theoretical realization.

• **Chapter 2:** describes the experimental techniques, structure, morphology, and composition employed in this work. Introduction of dc magnetisation and ac magnetic susceptibility measurements using a Superconducting Quantum Interference Device (SQUID), Small-Angle Neutron Scattering (SANS), and X-ray absorption spectroscopy (XAS) are presented.

• **Chapter 3:** presents magnetometry to study the low-temperature magnetic phase diagram of $NiBr_2$ single crystals in the vicinity of T_{IC} = 23 K and around the incommensurate phase. By covering a field range from 0.1 T to 3 T, the ac susceptibility reveals the characteristic relaxation associated with the transitions between the collinear and noncollinear phases, which shows the signature of the field-induced helimagnetic transition. The nature

of field-induced transition and microscopic features were analysed in Chapter 5, with a broad range of magnetic fields and small-angle neutron scattering experiments.

• **Chapter 4:** represents the extended range of ac & dc magnetometry with the applied magnetic field (1 -14 T) in a-b basal plane and out of the plane, complemented by SANS. The results demonstrate a clear view of the magnetic-field-induced non-collinear to collinear spin transition in the triangular spin-lattice of helimagnet $NiBr_2$ single crystals. Our experimental outcomes are closely related to Okubo *et al.* (PRL 108, 017206 (2012)), where the formation of multi-q states and the skyrmions phase for a triangular spin-lattice has been suggested. This study searched for these states in $NiBr_2$ single crystals, but could not find any signature of the skrmionic phase in the $NiBr_2$ single crystal. Instead, a typical degeneracy occupation of the equivalent wave vector for the incommensurate state was detected.

• **Chapter 5:** In this chapter, the structural, electronic, and magnetic properties of Cd-doped Cu_2OSeO_3 nanocrystallites are described. In addition, cost-effective and fast synthesis of Cu_2OSeO_3 nanocrystallites with sizes ranges over 50-200 nm. The physical significance of Cd doping on the Cu_2OSeO_3 skyrmions will carry significant technological importance, as doping-induced chemical pressure can be used to tune and control the skyrmionic phases and their various physical properties.

• **Chapter 6:** presents the influence of Mn-doping on structural and magnetic properties of canted antiferromagnet $SmFeO_3$ single crystals obtained by optical float zone technique. SQUID magnetometry was performed in the temperature range from 5 to 400 K. The results reveal a new spin reorientation from the weak ferromagnetic state to the compensated antiferromagnetic state at nearly 180 K, which is missing in the parent compound for magnetic fields applied along with the different crystallographic directions due to Mn doping. Variations in the coercive field indicate the emergence of the exchange bias phenomenon at low temperatures. The microscopic origin of spin reorientations remains unclear.

• **Chapter 7:** Finally, in this chapter, concluding remarks are presented on the basis of the experimental findings and theoretical interpretation obtained in all the single crystal and nanocrystallite samples that are addressed in the thesis.